



Pergamon

Tetrahedron 56 (2000) 8095–8100

TETRAHEDRON

Conformational Analysis of the Cyclohexenone Ring in Abscisic Acid and its Analogs with a Fused Cyclopropyl Ring

Yasushi Todoroki^{a,*} and Nobuhiro Hirai^b^aDepartment of Applied Biological Chemistry, Faculty of Agriculture, Shizuoka University, Shizuoka 422-8529, Japan^bDivision of Applied Life Sciences, Graduate School of Agriculture, Kyoto University, Kyoto 606-8502, Japan

Received 17 July 2000; accepted 16 August 2000

Abstract—The conformational behavior of the cyclohexenone ring in abscisic acid (**1**) and its analogs (**2–5**) with a fused cyclopropyl ring was investigated by a low-temperature NMR analysis and computer-aided calculations of the model compounds. The ¹H signals of **1** separated into two sets below 250 K, which was a coalescence temperature, in a 99.4:0.6 ratio at 185 K, although the small set of signals was not complete. The large and small sets of signals were considered to correspond to an envelope **1-i** with the axial side-chain and another envelope **1-ii** with the equatorial side-chain. At 185 K, the free-energy barrier for the ring inversion between **1-i** and **1-ii** was determined to be ca. 11 kcal/mol, and the free-energy difference between the two conformers was ca. 1.4 kcal/mol. The ¹H signals of **2–5** never broadened even at 200 K, suggesting that these analogs are more flexible than **1**. These experimental results were consistent with those obtained by calculations using models **6–10**. Introducing a cyclopropyl group into the ring of **1** lowered the energy barrier for ring inversion and varied the conformational ratio at equilibrium between the minimum-energy conformers. © 2000 Elsevier Science Ltd. All rights reserved.

Introduction

The plant hormone abscisic acid (ABA, **1**) is a sesquiterpene that is involved in the regulation of many physiological processes such as the enhancement of adaptation to various stresses.¹ The mechanism of action of **1**, including its initial perception by target cells via receptors, is not well understood. An understanding of the three-dimensional shape required for its biological activities, as well as localized structure–activity relationships, which have been well investigated albeit only qualitatively,² will be essential for designing an effective probe for identifying ABA receptors and a highly active ABA analog.

The structure of **1** consists of a cyclohex-2-enone and five substituents including the 3-methyl-2,4-pentadienoic acid side-chain (Fig. 1). Cyclohex-2-enone itself is relatively flat, so the three-dimensional shape of **1** depends largely on the orientations of the substituents, which change in the conformation of the ring. The conformational behavior of cyclohex-2-enone has been investigated less than those of cyclohexane and cyclohexene, but the minimum-energy conformer seems to be an envelope or half-chair, as with cyclohexene.³ Although the transition state in the inversion of cyclohexenone has never been investigated, it may be close to a boat based on analogy to cyclohexene.⁴

The cyclohexenone ring of **1** can theoretically have at least two minimum-energy conformers; one is an envelope (or half-chair) with the axial side-chain, **1-i**, and the other is an inverted envelope (or half-chair) with the equatorial side-chain, **1-ii** (Fig. 1).⁵ The crystal structure that has been reported for **1**⁶ reveals that its ring is **1-i**, and NOE experiments have suggested that the ring of **1** adopts the envelope form **1-i** in solution.⁷ However, this does not exclude the possibility of any other conformers, since the ring of **1** is flexible. Since the barrier to interconversion for a cyclohexenone ring should be as low as that for a cyclohexene ring,⁴ any conformation in preferred conformational processes can be the active conformation if it realizes the lowest-energy complex with the receptor. The most effective ligand molecule should be that which can adopt such a conformation with the least cost in free-energy.

Milborrow proposed the hypothesis that the active conformation of **1** adopts the ring **1-ii**.⁸ Perras et al. recently demonstrated that the conformer with **1-ii** is preferable to that with **1-i** in the binding site of the uptake carrier.^{9,10} This demonstration depends on the strong activity of analogs in which the side-chain is fixed in or prefers the equatorial-like orientation.¹¹ However, there are some exceptions, and Milborrow's hypothesis has never been proven in relation to biological activity.

To determine the biologically active conformation, in a previous study, we synthesized and assayed four fused-type bicyclic ABA analogs **2–5** which had a cyclopropyl ring at the C-2'–C-3' or C-5'–C-6' in ABA (Fig. 2).¹² This

Keywords: conformation; cyclohexenones; cyclopropanes; computer-assisted methods.

* Corresponding author. Tel./fax: +54-238-4871; e-mail: aytodor@agr.shizuoka.ac.jp

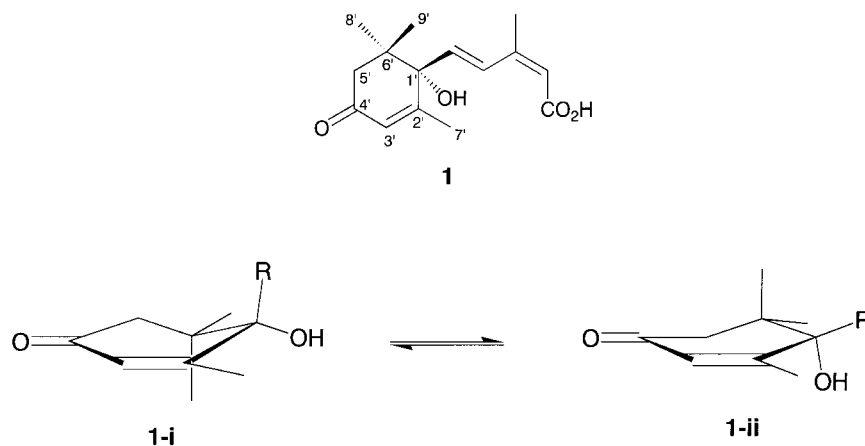


Figure 1. Structural formula and ring conformations of **1**.

modification has little effect on spoil the functional groups which are necessary for the biological activity of **1**. This is an advantage in identifying conformation–activity relationships. These bicyclic analogs are good probes because such minimum modification results in a variety of biological activities depending on whether cyclopropane was introduced to the upper or lower side of the cyclohexenone ring, suggesting that the changes in activity are caused by changes in conformational properties. In this report, we describe low-temperature ^1H NMR studies and computer-aided calculations for **1**, the bicyclic ABA analogs **2–5** and their models **6–10** to demonstrate the conformational requirements of the ring for the biological activity of **1**.

Experimental and Computational Methods

Compound **1** (synthetic racemate) was purchased from Tokyo Kasei Kogyo Co., Ltd and used as received. The synthesis of analogs **2–5** has been reported previously.¹² The atoms of all of the compounds including model compounds **6–10** were numbered as in **1** to avoid unnecessary confusion.

The ^1H NMR spectra were recorded on a Bruker ARX500 (500.13 MHz) from 300 to 185 K for **1** and from 300 to 200 K for **2–5**. NMR samples were prepared in 5-mm thin-walled NMR tubes as 0.07 M solutions in acetone- d_6 . A small amount of TMS was added to each sample as an internal reference. None of the samples were spun.

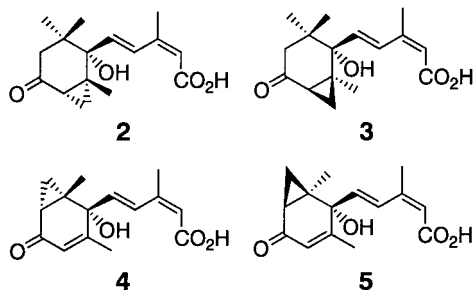


Figure 2. Four bicyclic ABA analogs with a cyclopropyl ring: **2**: 2' α ,3' α -dihydro-2' α ,3' α -methano-ABA; **3**: 2' β ,3' β -dihydro-2' β ,3' β -methano-ABA; **4**: 5' α ,8'-cyclo-ABA; **5**: 5' β ,9'-cyclo-ABA.

The rate constant for **1** at 250 K, 793 s^{-1} , was obtained by multiplying the separation of the signals of H-5'-*proR* at 185 K by 2.22.¹³ The free energy of activation, 11.2 kcal/mol, was calculated based on the Eyring equation using the rate constants.

All of the minimum-energy conformers of models **6–10** were generated and minimized using MM3 combined with the molecular dynamics simulation built into CAChe 3.11.¹⁴ The conformational energy surfaces in the C1'–C5 and C1'–O bond rotations were examined using MM3, where the dihedral angles C(4)C(5)C(1')O(1') and C(5)C(1')O(1')H were changed from -180 to 180° in 10-degree increments. The minimum-energy geometries were abstracted and further minimized without freezing the dihedral angles using MM3. These MM3-minimized structures were fully optimized with density functional theory, using the Becke three parameter hybrid functional (B3LYP) method and the 6-31G(d) basis set in GAUSSIAN 98,¹⁵ followed by a calculation of the harmonic vibrational frequencies at 298 K at the same level. Transition geometries for the ring inversion process for models **6–8** were preliminarily examined by PM3 in CAChe 3.11, where the dihedral angles ϕ_1 [C(2')C(1')C(5')C(6')] and ϕ_2 [C(3')C(4')C(5')C(6')] were chosen as the driving parameters for the interconversion process. Transition geometries (saddle points) for the ring inversion of **6–8** were found in the conformational space for which ϕ_1 is nearly 0° (1,3-diplanars) ($\phi_2 > 0^\circ$: axial side-chain; $\phi_2 < 0^\circ$: equatorial side-chain). These saddle points were optimized by a quasi-Newton method at the B3LYP/6-31G(d) level, followed by a calculation of the harmonic vibrational frequencies at 298 K at the same level. A single imaginary frequency was found for each calculation. The displacements for the normal mode corresponding to the imaginary frequency were large at the carbons associated with the change in the ring conformation. All of the minimum-energy conformers of **1** were generated and minimized using MM3, as model **6**.

Results and Discussion

Low-temperature NMR studies of **1–5**

All of the ^1H signals of **1** broadened below than 300 K, and

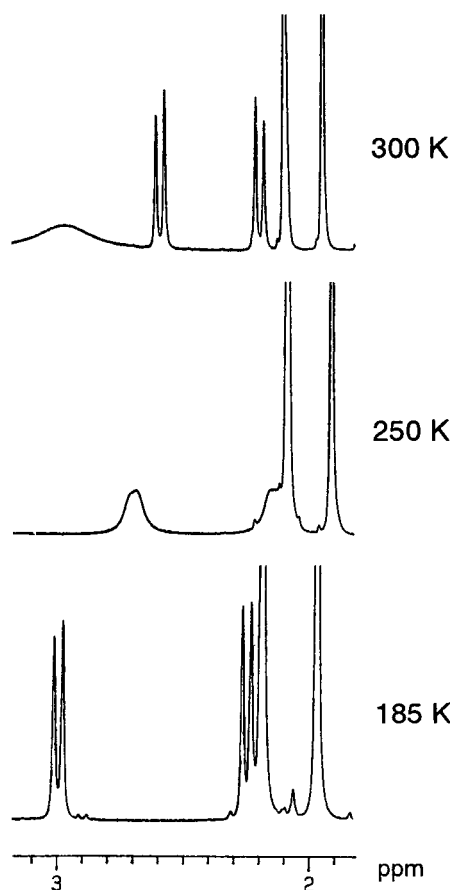


Figure 3. ^1H NMR spectra of **1** in acetone- d_6 .

the coalescence temperature was 250 K.¹⁶ As the temperature fell below 250 K, the signals grew sharper again and the signals split into the large and very small signals of the two corresponding conformers. This broadening of the signals

was the most remarkable at the 5'-protons (Fig. 3), indicating that the greatest difference in the chemical shifts between the two conformers occurred at the 5'-protons. The interconversion of the ring in **1**, from **1-i** to **1-ii**, reverses the orientation of the 5'-protons; the axial proton becomes the equatorial and the equatorial proton becomes axial. The axial proton at the α -position of the carbonyl group in many cyclohexanone derivatives appears at a lower field than an equatorial one.¹⁷ This should also be the case for the 5'-protons in **1**. The signal of the 5'-*proS* proton of **1-i** should appear at a lower field than that of the 5'-*proR* proton, and the signal of the 5'-*proS* proton of **1-ii** should appear at a higher field than that of the 5'-*proR* proton. Thus, it is reasonable to assume that the signal-broadening observed was caused by slow exchange between **1-i** and **1-ii**, rather than among rotational isomers of the side-chain or hydroxyl group. NOE experiments of **1** showed that the 5'-proton at a lower field had an NOE for the 5-proton.^{7a} Thus, the average signal of the 5'-*proS* proton from the two conformers appears at a lower field than that of the 5'-*proR* proton, suggesting that **1** exists predominantly as **1-i** rather than **1-ii**. In the separate signals, therefore, the large signals would correspond to **1-i** and the small ones would correspond to **1-ii**. The **1-i/1-ii** ratio based on integration of the signals was 99.4:0.6 at 185 K, meaning that the free-energy difference between the two conformers is 1.4 kcal/mol at this temperature. The free-energy barrier to interconversion between **1-i** and **1-ii** was calculated to be 11.2 kcal/mol from the rate constant (793 s^{-1}) at 250 K.

The ^1H signals of **2–5** never broadened, even at 200 K, suggesting that these analogs are more flexible than **1**, i.e. their energy barrier for interconversion is lower than that of **1**.

Ratio of axial to equatorial side-chains

We performed all of the computational studies using the

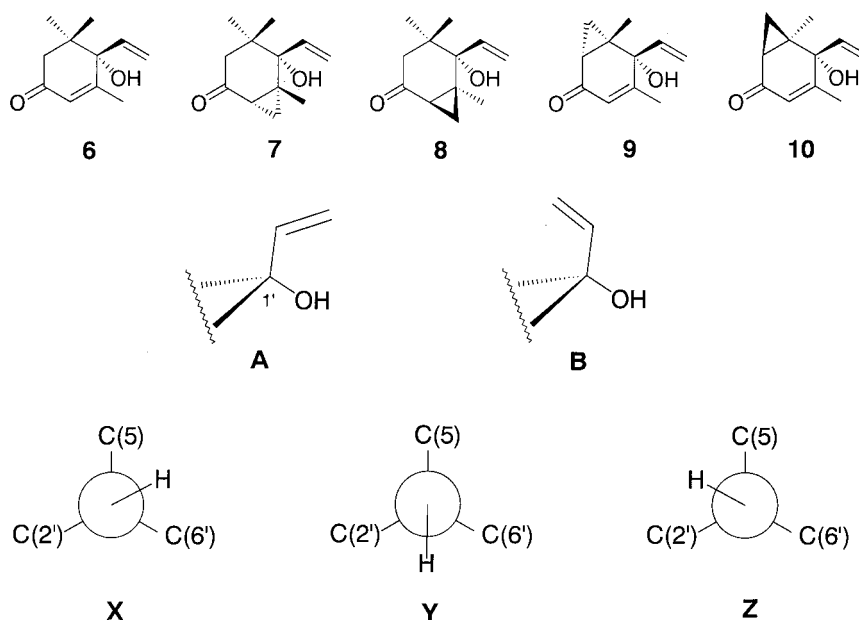


Figure 4. Model compounds **6–10** and their rotational isomers. Top: structural formula; middle: rotational isomers (A and B) with regard to C1'–C5 bond rotation; bottom: rotational isomers (X, Y and Z) with regard to O–C1' bond rotation.

Table 1. Relative B3LYP/6-31G(d) free energies of each minimum-energy conformer of **6–8**, and the side-chain axial/equatorial ratios

| Compound | Ring type ^a | Rotamers of the side-chain and hydroxy ^b | | | | | | Ratio of the axial/ equatorial side-chain |
|----------|------------------------|---|------|----------------|------|------|----------------|--|
| | | AX | AY | AZ | BX | BY | BZ | |
| 6 | i | 0.00 | 0.43 | 0.78 | 1.68 | 1.31 | 1.16 | 94.3:5.7 |
| | ii | 2.47 | 1.65 | 1.82 | 5.67 | 4.43 | 5.01 | |
| 7 | i | 4.48 | 4.23 | – ^c | 7.48 | 6.24 | – ^c | 0.1:99.9 |
| | ii | 0.88 | 0.00 | 0.00 | 6.42 | 5.08 | 5.08 | |
| | iii | 4.47 | 4.21 | 4.60 | 7.89 | 6.68 | 7.05 | |
| 8 | i | 0.00 | 0.70 | 2.42 | 3.83 | 4.52 | 4.71 | 59.0:41.0 |
| | ii | 1.23 | 0.87 | 0.77 | 3.36 | 2.88 | 2.88 | |
| | iv | 2.09 | 1.12 | 1.42 | 5.00 | 3.77 | 4.15 | |

^a **i**, envelope with the axial side-chain; **ii**, envelope with the equatorial side-chain; **iii**, boat with the axial side-chain; **iv**, boat with the equatorial side-chain.

^b See Fig. 4.

^c Not calculated because the conformation was not a minimum-energy geometry.

model compounds **6–10**, which have a vinyl group as a side-chain, to minimize computation time and exclude complexity caused by multiple conformations of the side-chain itself (Fig. 4). We examined the validity of applying the conformational behaviors of the model compounds to the parent compounds. All of the minimum-energy conformers of **1** were optimized using MM3, as was done later for model **6**. The free-energy difference between conformations of **1** with the axial and equatorial side-chains was very similar to that of **6**; the gap was only 0.1 kcal/mol. This suggests that simplification of the side-chain has little effect on the conformational behavior of the ring. Despite this simplification, we still have the complexity caused by rotation of the C1'–C5 and C1'–O bonds. We need to consider all of the local-minimum-energy geometries derived from the rotational isomers for the side-chain and hydroxyl group to estimate the distribution of the ring conformers with axial and equatorial side-chains. These rotational isomers can be divided into two types (A and B) with regard to C1'–C5 bond rotation and three types (X-, Y-, and Z) with regard to C1'–O bond rotation, to give six types overall: AX, AY, AZ, BX, BY, and BZ (Fig. 4). Each type of conformer was fully optimized using B3LYP after being pre-optimized using MM3 combined with a molecular dynamics simulation.

Table 1 shows the relative energy of each minimum-energy conformer of models **6–8** and the side-chain axial/equatorial ratios. At the minimum-energy points, the ring in **6** was one of two types: an envelope with the axial or equatorial side-chain, and each had six rotamers. The envelope conformers with the axial side-chain (**6-i**) had a lower energy than the corresponding conformers with the equatorial side-chain (**6-ii**). The axial/equatorial ratio was 94.3:5.7; the free energy difference was ca. 1.7 kcal/mol. This agreed with the experimental results. The two envelopes have two axial and three equatorial substituents. The two axial substituents are *anti*, whereas the three equatorial substituents are side-by-side. This means that the equatorial substituent in the ABA ring has a greater steric effect, which is referred to as allylic strain,¹⁸ than the axial substituent, which may help to explain why the lower-energy form is the envelope with a bulkier side-chain in comparison with the 1'-hydroxyl groups in the axial orientation. This is experimentally supported by the fact that the

1'-methyl ether of ABA prefers a conformation with the equatorial side-chain,⁹ probably because the bulky methyl ether favors the axial orientation.

For model **7**, the ring at the minimum-energy points could assume three forms; two envelopes with axial and equatorial side-chains (**7-i** and **7-ii**, respectively) and one boat with the axial side-chain (**7-iii**). The energy of model **7-ii** was lower than those of **7-i** and **7-iii**. The axial/equatorial ratio was 0.1:99.9; the free energy difference was 4.1 kcal/mol. The axial cyclopropyl ring in the envelope and boat with the axial side-chain is 1,3-diaxial for the methyl group (C-8'), which could explain why they are less stable than the envelope with the equatorial side-chain.

Model **8** also had three different types of ring at the minimum-energy points; two envelopes with axial and equatorial side-chains (**8-i** and **8-ii**) and one boat with the equatorial side-chain (**8-iv**). The axial/equatorial ratio was 59:41, and the free energy difference was almost zero. This may be due to the cyclopropyl ring which is *syn* to the side-chain. The axial side-chain would be repulsive to the cyclopropyl ring.

Models **9** and **10** had only one type of ring at the minimum-energy point because of the 1,4-cyclohexadiene-like

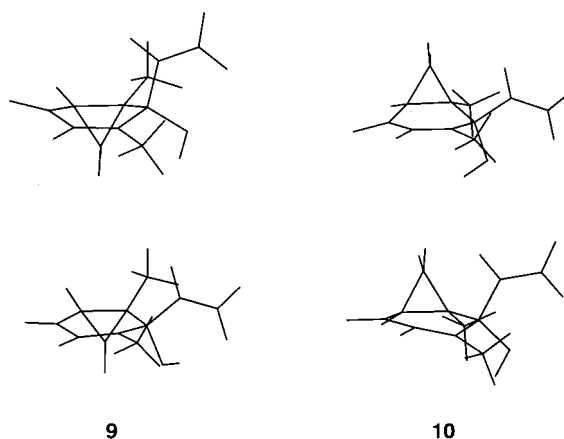


Figure 5. Minimum-energy conformations of **9** and **10** (upper), and unfavorable conformations with the orientation of the side-chain frozen (lower).

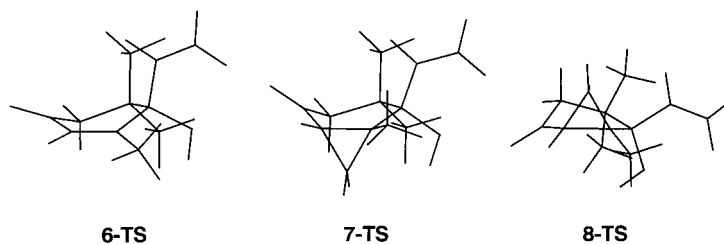


Figure 6. Transition-state structures for ring inversion of 6–8.

structure.¹⁹ The minimum-energy ring of **9** was a boat with the axial side-chain, while that of **10** was a boat with the equatorial side-chain. Since the C5'–C6' single bond in **9** and **10** is like a double bond due to the formation of a cyclopropyl ring,²⁰ ring puckering has little influence on the orientation of C-8' and C-9'. For **9**, therefore, the equatorial side-chain always results in greater steric hindrance for C-9', and for **10** the axial side-chain yields high steric energy for the axial C-9'. This is why **9** and **10** prefer axial and equatorial side-chains, respectively. A boat–boat inversion potential for **9** and **10** was calculated by partial optimization of the geometry in which the side-chain was frozen at an unfavorable orientation; the dihedral angle C(3')C(2')C(1')C(5) was fixed at 144° for **9** and at 96° for **10** (Fig. 5). Type AX and type AY were used for **9** and **10**, respectively, to calculate the most stable rotamer. We found that ca. 8 kcal/mol of free-energy was needed to adopt the side-chain orientation that **9** and **10** do not favor. This value was larger than that expected from the boat–boat inversion potential of 1,4-cyclohexadiene.¹⁹ This may be because of the sterically large substituents. Thus, the rings in **9** and **10** should exist mostly as boats with the axial and equatorial side-chains, respectively.

Barrier for ring interconversion

In examining the conformational space of models 6–8, we considered only AX or AY isomers, which should be more stable than the other types (see Table 1). The conformational space was searched at the PM3 level using two parameters for the dihedral angles ϕ_1 [C(2')C(1')C(6')C(5')] and ϕ_2 [C(3')C(4')C(5')C(6')]. The structures obtained for the minimum-energy and transition geometries were optimized at the B3LYP/6-31G(d) level.

For model compound **6**, the lowest-energy transition-state geometry was **6-TS**, which has the axial side-chain (Fig. 6). The B3LYP free-energy barrier at 298 K for ring inversion from **6-i-AX** to **6-TS** is 11.7 kcal/mol. This is consistent with that (11.2 kcal/mol) obtained in the low-temperature NMR analysis of **1**. This barrier is similar to that for cyclohexane (ca. 12 kcal/mol),²¹ meaning that this is a very flexible system. The lowest-energy transition state for ring inversion of **7** was **7-TS**, which has the axial side-chain (Fig. 6). The B3LYP free-energy barrier from **7-ii-AY** to **7-TS** was 8.6 kcal/mol. These values are smaller than those of **6** by 3 kcal/mol, meaning that this ring system is more flexible than that of **6**. This agrees with the above result that coalescence of the ¹H signals was not observed, even at 200 K, in the low-temperature NMR analysis of **2**. For ring inversion of **8**, the 1,3-diplanar **8-TS** with the equatorial side-chain was the lowest-energy transition state (Fig. 6). The

B3LYP free-energy barrier from **8-i-AX** to **8-TS** was 5.0 kcal/mol, which is smaller than that of **6** by 7 kcal/mol. This implies that this ring system undergoes interconversion more rapidly than **6**, just like **7**.

The above findings indicate that introducing a cyclopropyl group into the cyclohexenone ring of **1** lowers the energy barrier for ring inversion independent of the orientation of cyclopropane. On the other hand, the minimum-energy geometries or their conformational ratio at equilibrium changed dramatically according to the orientation of the cyclopropane; the population of the conformer with the axial side-chain is over 99% for **6** and **9**, 59% for **8**, and below 1% for **7** and **10** on the basis of B3LYP calculations. These results should be applicable to parent compounds **1–5:1** and **4** should almost certainly adopt the axial side-chain; **2** and **5** should have the equatorial side-chain; and **3** should have both. These results are related to their biological activities. The concentration that inhibits stomatal opening by 50% is 3 nM for **1** and **4**, 130 nM for **3**, and over 1000 nM for **2** and **5**.^{12,22} This strongly suggests that the ring conformation of **1** in a complex with receptors is close to an envelope with the axial side-chain.

References

1. *Abscisic Acid*, Davies, W. J., Jones, H. G. Eds.; BIOS: Oxford, 1991.
2. Walton, D. C. *Abscisic Acid*; Addicott, F. T. Ed.; Praeger: New York, 1983, pp 113–146.
3. Microwave studies, Raman spectra, and theoretical methods have suggested an envelope rather than a half-chair conformation in the gas phase (Abraham, R. J.; Lucas, M. S. *J. Chem. Soc. Perkin Trans. II* **1988**, 669–672 and references cited therein).
4. Some reports have indicated that cyclohexene gives 5–10 kcal/mol (Laane, J.; Choo, J. *J. Am. Chem. Soc.* **1994**, *116*, 3889–3891 and references cited therein). Substitution of a methylene group for a carbonyl will lead to the elimination of torsional strain during ring inversion, so cyclohex-2-enone should have a lower barrier than cyclohexene.
5. Although the terms pseudo-axial and quasi-equatorial have been frequently used to define substituent positions in cyclohexene, we use the terms axial and equatorial according to the Cremer's definition to avoid such vague terms (Cremer, D.; Szabo, K. J. *Conformational Behavior of Six-membered Rings*; Juaristi, E., Ed., VCH: New York, 1995; pp 59–135).
6. (a) Ueda, H.; Tanaka, J. *Bull. Chem. Soc. Jpn* **1977**, *50*, 1506–1509. (b) Schmalle, V. H. W.; Klaska, K. H.; Jarchow, O. *Acta Crystallogr.* **1977**, *B33*, 2218–2224.
7. (a) Milborrow, B. V. *Biochem. J.* **1984**, *220*, 325–332. (b)

- Willows, R. D.; Milborrow, B. V. *Phytochemistry* **1993**, *34*, 233–237.
8. Milborrow, B. V. *Plant Growth Substances*; Bopp, M. Ed.; Springer: Berlin, 1986, pp 108–119.
9. Perras, M.; Rose, P. A.; Pass, E. W.; Chatson, K. B.; Balsevich, J. J.; Abrams, S. R. *Phytochemistry* **1997**, *46*, 215–222.
10. The existence of a saturable component in the uptake of ABA into cells has been well documented (reference 9 and references cited therein). ABA can permeate cell membranes and the ABA receptor is believed to be located on the outer face of the plasma membrane, although the possibility of an intracellular receptor has never been excluded (For the extracellular receptor: Anderson, B. E.; Ward, J. M.; Schroeder, J. I. *Plant Physiol.* **1994**, *104*, 1177–1183. Gilroy, S.; Jones, R. L. *Plant Physiol.* **1994**, *104*, 1185–1192. For the intracellular receptor: Allan, A. C.; Fricker, M. D.; Ward, J. L.; Beale, M. H.; Trewavas, A. *J. Plant Cell* **1994**, *6*, 1319–1328. Schwartz, A.; Wu, W.-H.; Tucker, E. B.; Assmann, S. M. *Proc. Natl. Acad. Sci. USA* **1994**, *91*, 4019–4023). Thus, the role of the uptake carrier is unknown. The fact that the activity of uptake has never been correlated with biological activity complicates this subject (Windsor, M. L.; Milborrow, B. V.; Abrams, S. R. *J. Exp. Bot.* **1994**, *45*, 227–233).
11. For example, (+)-2,3-dihydro-ABA, which adopts the axial side-chain, very effectively inhibits the uptake of ABA.⁹
12. Todoroki, Y.; Nakano, S.; Hirai, N.; Ohigashi, H. *Tetrahedron* **1996**, *52*, 8081–8098.
13. (a) Günther, H. *NMR Spectroscopy*, 2nd ed.; Wiley: Chichester, 1995; pp 335–389. (b) Juaristi, E. *Introduction to Stereochemistry and Conformational Analysis*; Wiley: Chichester, 1991, pp 253–270.
14. CAChe, 3.11, 1998 Oxford Molecular Ltd. The version of MOPAC is 94. 10 derived from 6.00.
15. Frisch, M. J.; Trucks, G. W.; Schlegel, H. B.; Scuseria, G. E.; Robb, M. A.; Cheeseman, J. R.; Zakrzewski, V. G.; Montgomery, Jr., J. A.; Stratmann, R. E.; Burant, J. C.; Dapprich, S.; Millam, J. M.; Daniels, A. D.; Kudin, K. N.; Strain, M. C.; Farkas, O.; Tomasi, J.; Barone, V.; Cossi, M.; Cammi, R.; Mennucci, B.; Pomelli, C.; Adamo, C.; Clifford, S.; Ochterski, J.; Petersson, G. A.; Ayala, P. Y.; Cui, Q.; Morokuma, K.; Malick, D. K.; Rabuck, A. D.; Raghavachari, K.; Foresman, J. B.; Cioslowski, J.; Ortiz, J. V.; Stefanov, B. B.; Liu, G.; Liashenko, A.; Piskorz, P.; Komaromi, I.; Gomperts, R.; Martin, R. L.; Fox, D. J.; Keith, T.; Al-Laham, M. A.; Peng, C. Y.; Nanayakkara, A.; Gonzalez, C.; Challacombe, M.; Gill, P. M. W.; Johnson, B.; Chen, W.; Wong, M. W.; Andres, J. L.; Gonzalez, C.; Head-Gordon, M.; Replogle, E. S.; Pople, J. A. GAUSSIAN 98, Revision A.3, Gaussian, Inc., Pittsburgh PA, 1998.
16. Perras, et al.¹⁰ reported that the signals of ABA (in CD₃CD₂OD) and its methyl ester (in CDCl₃ and CD₃CD₂OD) were not separated in low-temperature NMR (500 MHz, 300–175 K). We cannot conclusively explain this discrepancy. A possible explanation is that different solvents have different effects on minima and saddle points. Chloroform and ethanol may stabilize saddle points rather than minima to lower the energy barrier for ring inversion.
17. Jackman, L. M.; Sternhell, S. *Applications of Nuclear Magnetic Resonance Spectroscopy in Organic Chemistry*, 2nd ed.; Pergamon Press: Oxford, 1969 (pp 238–241).
18. Johnson, F. *Chem. Rev.* **1968**, *68*, 375–413.
19. (a) Jeffrey, G. A. *J. Am. Chem. Soc.* **1988**, *110*, 7218–7219. (b) Birch, A. J.; Hinde, A. L.; Radom, L. *J. Am. Chem. Soc.* **1981**, *103*, 284–289. (c) Oberhammer, H.; Bauer, S. H. *J. Am. Chem. Soc.* **1969**, *91*, 10–16.
20. (a) Hamilton, J. G.; Palke, W. E. *J. Am. Chem. Soc.* **1993**, *115*, 4159–4164. (b) Wong, H. N. C.; Hon, M.-Y.; Yse, C. W.; Yip, Y. C.; Tanko, J.; Hudlicky, T. *Chem. Rev.* **1989**, *89*, 165–198.
21. Bushweller, C. H. *Conformational Behavior of Six-membered Rings*; Juaristi, E. Ed.; VCH: New York, 1995, pp 25–58.
22. Since the stomatal-opening assay is a short-term assay (3 h), the activity of an ABA analog will be affected very little by the rate of its metabolism. Its uptake into cells by the carrier can also be downplayed because ABA would be detected by outward-facing plasma membrane receptors with respect to the inhibition of stomatal opening (Anderson, B. E.; Ward, J. M.; Schroeder, J. I. *Plant Physiol.* **1994**, *104*, 1177–1183). This means that this assay is suitable for evaluating the binding of ABA analogs to receptors.